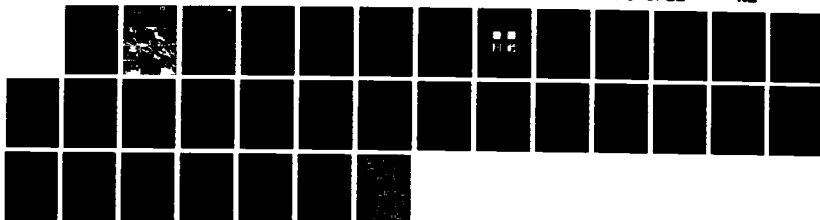AD-A194 988

MECHANICAL PROPERTIES OF MULTI-YEAR SEA ICE PHASE 2 ICE   1/1
STRUCTURE ANALYSIS(U) COLD REGIONS RESEARCH AND
ENGINEERING LAB HANOVER NH J RICHTER-MENGE ET AL.
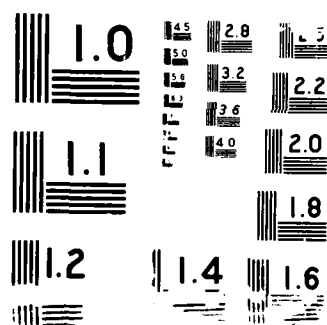
UNCLASSIFIED   MAR 88 CRREL-88-5   F/G 8/12   NL

CRREL
REPORT 88-5

US Army Corps of Engineers

Cold Regions Research &
Engineering Laboratory

Mechanical properties of multi-year sea ice
Phase II: Ice structure analysis

88 5 16 087

CRREL Report 88-5

March 1988

Mechanical properties of multi-year sea ice
Phase II: Ice structure analysis

Jacqueline Richter-Menge and Nancy M. Perron

Accession For

NTIS CRA&I

DTIC TAB

Unannounced

Justification

By

Distribution

Availability

Dist

A-1

REPORT DOCUMENTATION PAGE

Form Approved
OMB No 0704-0188
Exp Date Jun 30, 1986

1a. REPORT SECURITY CLASSIFICATION Unclassified	1b. RESTRICTIVE MARKINGS
2a. SECURITY CLASSIFICATION AUTHORITY	3. DISTRIBUTION/AVAILABILITY OF REPORT Approved for public release; distribution is unlimited.
2b. DECLASSIFICATION/DOWNGRADING SCHEDULE	

4. PERFORMING ORGANIZATION REPORT NUMBER(S) CRREL Report 88-5	5. MONITORING ORGANIZATION REPORT NUMBER(S)

6a. NAME OF PERFORMING ORGANIZATION U.S. Army Cold Regions Research and Engineering Laboratory	6b. OFFICE SYMBOL (If applicable) CECRL	7a. NAME OF MONITORING ORGANIZATION See 16.

6c. ADDRESS (City, State, and ZIP Code) Hanover, New Hampshire 03755-1290	7b. ADDRESS (City, State, and ZIP Code)

8a. NAME OF FUNDING/SPONSORING ORGANIZATION	8b. OFFICE SYMBOL (If applicable)	9. PROCUREMENT INSTRUMENT IDENTIFICATION NUMBER

8c. ADDRESS (City, State, and ZIP Code)	10. SOURCE OF FUNDING NUMBERS			
	PROGRAM ELEMENT NO.	PROJECT NO.	TASK NO.	WORK UNIT ACCESSION NO

11. TITLE (Include Security Classification)
Mechanical Properties of Multi-Year Sea Ice
Phase II: Ice Structure Analysis

12. PERSONAL AUTHOR(S)
Richter-Menge, Jacqueline and Perron, Nancy M.

13a. TYPE OF REPORT	13b. TIME COVERED FROM _____ TO _____	14. DATE OF REPORT (Year, Month, Day) March 1988	15. PAGE COUNT 32

17.	COSATI CODES		18. SUBJECT TERMS (Continue on reverse if necessary and identify by block number)
FIELD	GROUP	SUB-GROUP	Ice Mechanical properties
			Ice properties Sea ice
			Ice structure

19. ABSTRACT (Continue on reverse if necessary and identify by block number)
This report describes the structural analysis of multi-year sea ice samples that were tested in the second phase of a program designed to obtain a comprehensive understanding of the mechanical properties of multi-year sea ice from the Alaskan Beaufort Sea. Each test specimen is classified into one of three major ice texture categories: granular, columnar, or a mixture of columnar and granular ice. The crystallographic orientation, percent columnar ice, and grain size are then evaluated for the granular and/or columnar ice in the sample. Test results are interpreted with respect to these parameters. The overall composition of multi-year ridges is considered, based on the extensive field sampling that was done in the program. The effect of sample orientation on the results is also discussed.

20 DISTRIBUTION/AVAILABILITY OF ABSTRACT ☒ UNCLASSIFIED/UNLIMITED ☐ SAME AS RPT ☐ DTIC USERS	21 ABSTRACT SECURITY CLASSIFICATION Unclassified
22a. NAME OF RESPONSIBLE INDIVIDUAL Jacqueline Richter-Menge	22b TELEPHONE (Include Area Code) 603-646-4100 22c OFFICE SYMBOL CECRL-RS

DD FORM 1473, 84 MAR   83 APR edition may be used until exhausted
All other editions are obsolete

SECURITY CLASSIFICATION OF THIS PAGE
Unclassified

PREFACE

CONTENTS

ILLUSTRATIONS

TABLES

Mechanical Properties of Multi-Year Sea Ice
Phase II: Ice Structure Analysis

JACQUELINE RICHTER-MENGE AND NANCY M. PERRON

INTRODUCTION

This report presents the ice structure analysis of multi-year pressure ridge samples tested in the second phase of a joint government–industry study. The study was initiated to examine systematically the structure and mechanical properties of ice samples taken from multi-year ridges. Interest in the properties of multi-year ridges stems from the fact that these ridges are the most frequently encountered, massive ice features in exposed areas of the Beaufort and Chukchi Seas. Deep-water oil platforms constructed in this area of the arctic must be designed, therefore, to withstand the impact of a multi-year ridge.

Both Phase I and Phase II of this program involved field sampling in the southern Beaufort Sea. The Phase I field program was conducted in April 1981 and involved the sampling of 10 different pressure ridges. A continuous, vertical multi-year ridge core was also specifically obtained for detailed structural analysis. A total of 220 unconfined uniaxial constant-strain-rate compression tests were performed on the vertically cored ice samples from the 10 ridges. The preliminary ice structure analysis of these test specimens indicated that the main factor contributing to large variations in the test results was associated with the extreme local variability of ice structure within a ridge. It became apparent that a complete and useful analysis of the multi-year ridge ice property test data would require a thorough structural interpretation of each test sample.

Additional multi-year ice from four ridges was collected in April 1982 for the Phase II tests. These field samples included horizontally and vertically cored ice samples taken in close proximity to one another. The matched pairs were tested in unconfined, uniaxial constant-strain-rate compression to investigate the effect of sample orientation on the test results. The remaining vertical ice samples were used in additional unconfined

compression tests and in confined constant-strain-rate compression, constant-strain-rate tension, and constant load compression tests. A total of 188 tests were done in Phase II. During the Phase II field program, we also extracted a second vertically drilled continuous ridge core to augment the ice structure data obtained in Phase I.

This report includes the ice structure analysis of the Phase II multi-year pressure ridge test specimens with the exception of the constant load compression tests. We have also included the analysis of the continuous ridge core taken during the second field program. The structural analysis of the ice samples tested in Phase I is presented in Richter-Menge et al. (1987). Discussions on the field sampling program and the test results and analyses for Phases I and II can be found in Cox et al. (1984, 1985, respectively).

SAMPLE ANALYSIS

The structural characteristics of the continuous multi-year ridge core and the Phase II ridge test specimens were evaluated using the same techniques described in Richter-Menge et al. (1987). Briefly, ice thin sections were prepared from the sample after testing (Fig. 1). If a sample was destroyed during the test, end pieces taken immediately adjacent to the test specimen were used to interpret the structural composition of the sample. The ice type was determined by studying the photographs taken of the thin sections in crossed polaroid light.

The ice type of each sample was described according to the multi-year pressure ridge ice structural classification scheme summarized in Table 1. Figure 2 shows a series of thin sections, photographed between crossed polarizers, that illustrates the principal structural characteristics of each ice type. This structural classification scheme divides the ice into three major ice-texture categor-
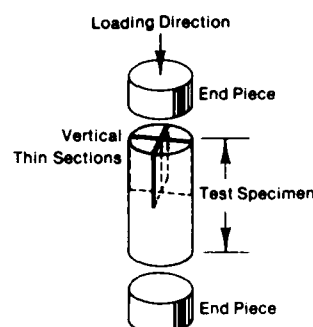
Figure 1. Sections used in the analysis of the structural characteristics of the tested ice samples.

Table 1. Structural classification scheme for multi-year pressure ridge ice samples.

Ice type	Code	Structural characteristics
Granular	I	Isotropic, equiaxed crystals
Columnar	II	Elongated, columnar grains
	IIA	Columnar sea ice with c-axes normal to growth direction; axes may or may not be aligned
	IIC	Columnar freshwater ice
Mixed	III	Combination of Types I and III
	IIIA	Largely Type II with granular veins
	IIIB	Largely Type I with inclusions of Type II ice (brecciated ice)
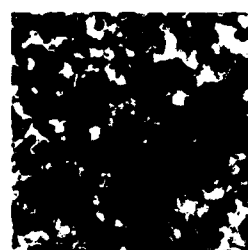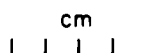
Figure 2. Structural characteristics of multi-year ice types.

ies: granular, columnar, or a mixture of columnar and granular ice. If a sample was classified as columnar or contained large ($\geq$ 10 cm) fragments of columnar ice, the ice thin sections were analyzed on the Rigsby universal stage (Langway 1958). Using these measurements we defined the mean angle between the crystallographic c-axes and the load direction (σ:c) and the degree of alignment of the c-axes (° spread).

We also used the thin section analysis to determine the angle between the columns, or direction of elongation of the crystals, and the load (σ:z). In an undeformed sheet of first-year sea ice the crystals are elongated vertically (σ:z = 0°), parallel to the growth direction of the sheet. The c-axes of these crystals are usually located in the horizontal plane of the ice sheet, normal to the elongation direction of the crystals. By observing the orienta-

2

tion of the crystallographic c-axes and the direction of elongation of the crystals in the ridge samples, we can determine the arrangement of some of the columnar fragments of first-year sea ice that have been incorporated into a ridge. The photographed thin sections of each sample helped to confirm these measurements.

Note that all of our samples, both horizontally and vertically cored, were cylindrical. The compressive or tensile load was applied along the cylindrical axis of the samples. For vertically cored samples then, σ:z also represents the angle between the direction of elongation and the vertical. Thin sections taken perpendicular to the load were used for the crystallographic measurements to avoid misinterpretation as a result of apparent dip and plunge.

The granular ice in the thin sections was not analyzed on the universal stage because the grain size was too fine, averaging 1 mm in diameter. The granular ice was observed between crossed polarizers, and the crystals appeared to be randomly oriented.

The maximum, minimum, and mean grain sizes of the columnar and/or granular crystals in each sample were estimated by using the thin section photographs. Each photograph included a millimeter scale next to the thin section for grain-size analysis. The grain-size measurements in the tension tests were made at the location of the failure plane. Unlike the compression tests, the tension samples all failed via an extension mechanism. The failure plane was normal to the load and easily identified in the thin section photographs. For the compression test specimens, we based our grain-size measurements on the textural characteristics of the entire sample.
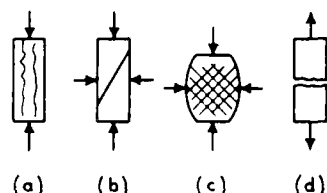
Figure 3. Typical failure modes. In compression: a) longitudinal splitting, b) shear fracture, and c) multiple shear fractures. In tension: d) extension fracture. (From Jaeger and Cook 1969.)

Backlighting was used to determine the gross structural features of the ice sample. Photographs of the sample at noted positions were taken before and after the test. The two sets of photographs were compared to distinguish between original and test-created ice textures in the unconfined and confined compression tests where the ice underwent considerable deformation. The post-test photographs of the sample were also used to determine the mode and location of the failure. The type of failure was described using Figure 3, taken from Jaeger and Cook (1969).

The Phase II continuous multi-year pressure ridge core was indexed with a vertical line along its entire length before thin sectioning. The core was then cut into 10-cm segments and thin-sectioned. A continuous structural profile of this core was prepared from the photographs taken of these thin sections between crossed polarizers. This structural profile is presented in Cox et al. (1985) together with a detailed description of the ice structure.

CONTINUOUS MULTI-YEAR RIDGE CORE

A schematic structural profile of the Phase II continuous vertical multi-year pressure ridge core is presented in Figure 4. Well-defined columnar zones in the core, indicated by the letter C, include a measurement of the angle between the direction of elongation of the crystals and the vertical (σ:z). We also note whether the crystal c-axes in the columnar ice were aligned or unaligned.

Nearly 50% of the ice in the Phase II core is columnar. The zones of columnar ice are distributed throughout the core, unlike the Phase I continuous core in which most of the columnar ice was concentrated at the bottom of the core. The remainder of the Phase II core is a combination of granular ice and mixed granular and columnar crystals. The mixed ice is predominately brecciated, composed of columnar fragments in a granular matrix. Based on these characteristics, it would appear that this multi-year ridge (ridge C) was initially formed by the compression of two adjacent ice sheets. We would anticipate a much lower percentage of columnar ice in a ridge formed by shearing.

As observed in the Phase I continuous ridge core and many of the Phase I test samples, the angle between the vertical and the direction of elongation of the crystals in the columnar zones of

Salinity (‰)

C, σ Z = 15°, Aligned
M
C, σ Z = 0°, Aligned at 110 cm
M
C, σ Z = 15°, Aligned
M
G
C, σ Z = 35°, Aligned
M
C, σ Z = 15°, Aligned
G
C, σ Z = 15°, Unaligned
M
C, σ Z = 15°, Unaligned

M

C; σ Z = 0°, Aligned at 900 cm (unaligned at bottom)

Figure 4. Salinity and schematic structural profile for the Phase II continuous multi-year pressure ridge core. G = granular ice, C = columnar ice, M = mixed granular and columnar ice.

Table 2. Columnar ice samples tested in Phase II, including both columnar and mixed samples with 80% or more columnar ice.

Test type	Ridge no.	Total samples tested	Total columnar samples	% columnar samples
Unconfined	A	9	0	0
compression	C	53	20	38
Confined	A	22	0	0
compression	B	33	7	21
Tension	A	15	1	7
	B	21	2	10
Total		153	30	20

tables since all of the samples failed via an extension mechanism (Fig. 3d). In Table 2, we have listed the total number of Phase II samples tested in each major loading state, noting the ridges that the samples were taken from and the number of columnar samples in each group.

Unconfined constant-strain-rate compression tests

The Phase II unconfined, uniaxial constant-strain-rate compression tests were done at two temperatures (-5 and -20°C) and two strain rates (10^{-2} and 10^{-4}/s). The test parameters were chosen to complement the unconfined constant-strain-rate compression tests done in Phase I at the same temperature, but at strain rates of 10^{-3} and 10^{-5}/s. Matched pairs of horizontally and vertically cored samples were tested at -5 and -20°C and a strain rate of 10^{-4}/s to determine the effect of sample orientation on the compressive strength of the multi-year ice. These samples were paired according to their location within the ridge. We have summarized the percent granular, columnar, and mixed ice samples at each test condition in Phase I and II in Table 3. As noted in the Phase I ice structure analysis report (Richter-Menge et al. 1987), the most common ice type by far is the mixed columnar and granular ice. Columnar ice was the dominant ice type at only one Phase II test condition: -20°C and 10^{-4}/s. The distribution of ice types is relatively consistent among all other test groups.

The compressive strength of the multi-year ridge samples is plotted against sample porosity and the structural classification is indicated for each test specimen in Figures 5a through d. We

the Phase II core is 15° or less. There is only one exception: at 350 cm, one section of columnar ice has a σ:z angle of 35°. This indicates that in ridge C, the columnar blocks were lying in a near-horizontal position (σ:z < 20°).

TESTED MULTI-YEAR RIDGE ICE SAMPLES

In this section we present the results of the ice structure analysis of the Phase II multi-year-ridge test specimens. Phase I results are included for comparison whenever it is appropriate. This additional data has helped us in the interpretation of the effect of ice structure on the Phase II test results. The structural classification and crystallographic measurements made on each Phase II test specimen are given in Appendix A. The samples are grouped according to test condition. The fracture mode for the tension tests is not listed in these

4

Table 3. Summary of percent granular, columnar, and mixed ice samples at each Phase I and Phase II unconfined compression test condition.

	-5°C				-20°C			
	$10^{-2}/s$	10^{-3}	10^{-4}	10^{-5}	10^{-2}	10^{-3}	10^{-4}	10^{-5}
Granular	0	7	0	10	11	3	0	2
Columnar	22	25	16 (20)	19	11	20	56 (46)	20
Mixed	78	68	84 (80)	71	78	77	44 (54)	78
Total samples tested	9	69	19 (9)	71	9	41	25 (13)	41

( ) Vertically cored samples only.

have also included all of the crystallographic data on the measured angle between the load and direction of elongation of the crystals (σ:z), the angle between the load and the mean crystallographic c-axis (σ:c), and the degree of alignment in the plane perpendicular to the elongation direction (° spread) for the columnar and mixed ice samples. The percentage of columnar ice in the sample is given for the mixed ice samples and for columnar ice samples that were not 100% columnar. We were unable to determine the percentage of columnar ice in the mixed ice samples for many of the $10^{-2}/s$ tests (Fig. 5a and c) since these samples were destroyed during the test. In Figures 5b and 5d, the horizontally cored samples are denoted.

In general, the influence of ice structure and crystal orientation on the unconfined compressive strength of the Phase II samples is similar to that described for the Phase I ice samples in Richter-Menge et al. (1987). At a strain rate of $10^{-4}/s$ and temperature of -20°C (Fig. 5d), the highest strength samples are composed of columnar ice with the direction of crystal elongation parallel to the load (σ:z $\leq$ 10°) and a relatively small degree of c-axis alignment ($\leq$ 50°). We again observe a rapid drop-off in the compressive strength of the columnar samples as σ:z increases from 0°. The mixed ice samples with a high percentage of columnar ice (80% or more) exhibit characteristics similar to the columnar ice samples. This is evident in the tests done at a strain rate of $10^{-4}/s$ and temperature of -5°C (Fig. 5b). These mixed ice samples lie on the perimeter of the strength vs porosity band. At all test conditions, 10^{-4} and $10^{-2}/s$, there is a tendency for the compressive strength of the mixed and granular ice samples to decrease with an increase in porosity. The influence of grain size on the compressive strength of the ridge samples appears insignificant compared to the effects of crystal orientation and porosity.

All of the matched sample pairs we tested were obtained from ridge C, the same ridge that provided the continuous ridge core described in the previous section. The tests done on the matched pairs (Fig. 5b and d) do indicate that the mean compressive strength of ice samples from a multi-year ridge is dependent on sample orientation. Vertically cored samples tend to give a higher mean strength than horizontally cored samples. The dependence of mean compressive strength on sample orientation can be explained by sample ice structure. The ice structure analysis of the ridges that we have sampled, including ridge C, suggests that most of the large columnar ice blocks in a multi-year ridge that was initially formed by compression lie in a near-horizontal position. At this orientation the direction of elongation of the crystals or the columns in these large ice blocks is near vertical. The columnar ice samples collected from vertical coring will therefore be loaded nearly parallel to the direction of crystal elongation (σ:z = 0°). This is the hard fail direction in columnar ice. Horizontally cored columnar ridge samples tend to have an angle of 90° between the long columns and the applied load (σ:z = 90°). Work by Peyton (1966) and Timco and Frederking (1986) has shown that columnar ice samples loaded parallel to the elongated crystal axes have compressive strengths 2 to 4 times higher than samples loaded normal to the direction of elongation. Mixed ice samples with large ($\geq$ 10-cm) fragments of columnar ice are also affected by the orientation of the columnar ice within them. If the columnar fragments in the sample are oriented with the direction of crystal elongation parallel to the load (σ:z = 0°), the sample will fail at a relatively high load and deformation will occur in the granular material surrounding the columnar fragments. The difference between the mean compressive strength of vertically and horizontally cored samples will depend on the

5
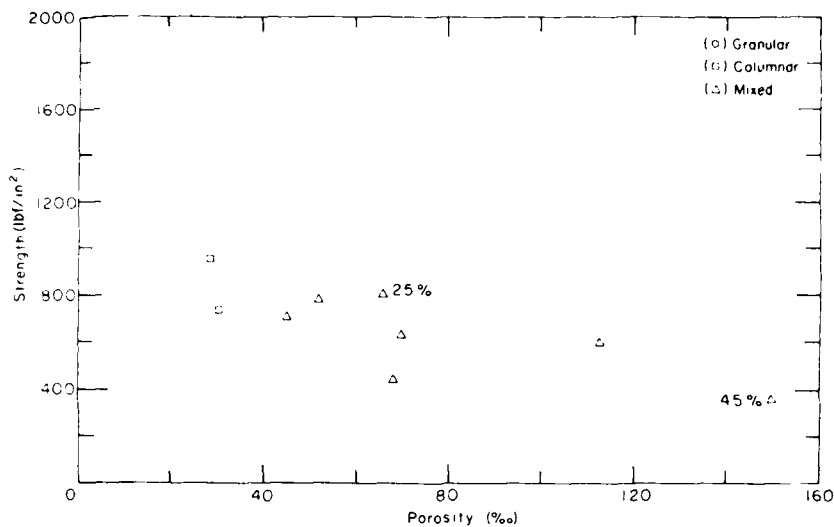
a. Tests conducted at $10^{-2}/s$ and $-5°C$.
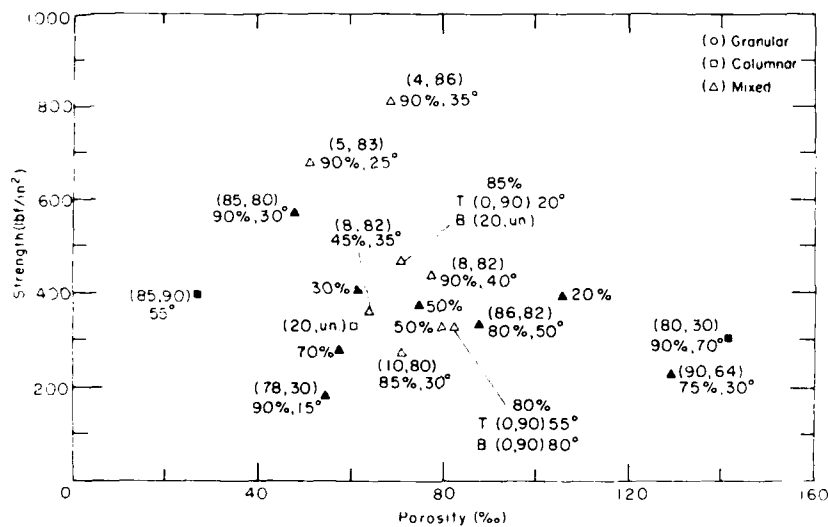
b. Tests conducted at $10^{-4}/s$ and $-5°C$.

Figure 5. Unconfined, constant-strain-rate compressive strength vs porosity for all Phase II ridge ice samples with the structural classification indicated for each sample. Open symbols = vertically cored samples; closed symbols = horizontally cored samples. Crystallographic measurements indicated next to each sample: (σ:z, σ:c), % columnar, ° spread.

number of columnar test specimens in the test series and their crystallographic orientation relative to the load. The results from the tests on the matched ridge ice sample pairs are discussed in more detail in Richter-Menge and Cox (1985).

The influence of the c-axis orientation relative to the load ($\sigma:c$) on the compressive strength of the columnar samples is evident in Figure 5d. The majority of horizontal samples tested at this condition were columnar and had an angle of approximately 90° between the direction of elongation and the load, which was applied along the cylindrical axis of the test specimen ($\sigma:z = 90°$). These horizontal samples had a higher strength when $\sigma:c$

6
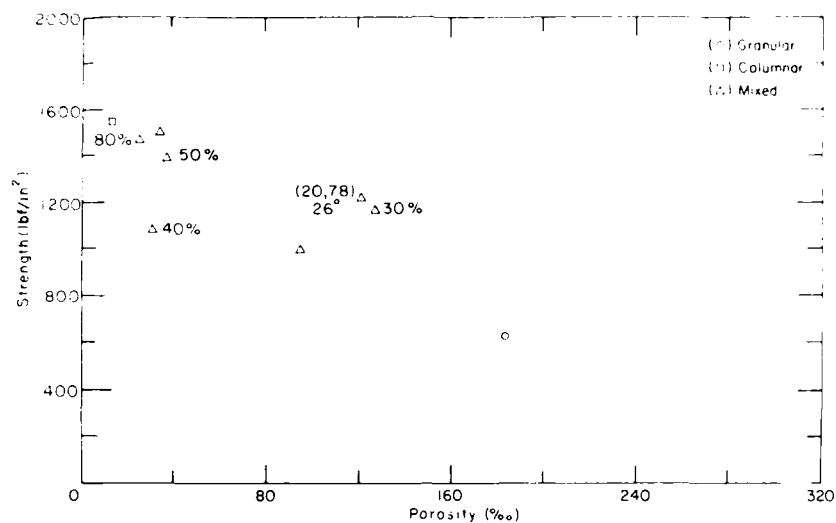
c. Tests conducted at 10^{-2}/s and $-20°C$.
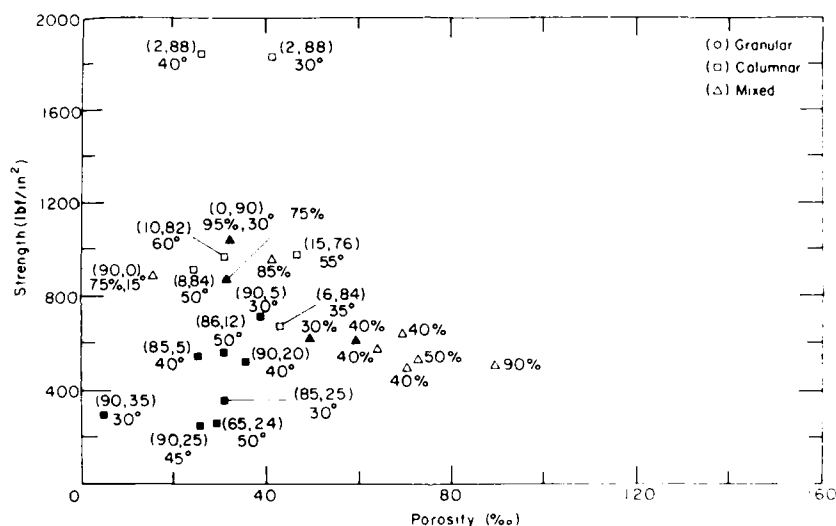
d. Tests conducted at 10^{-4}/s and $-20°C$.

Figure 5 (cont'd).

was near 0°. As the σ:c angle increased, the compressive strength decreased significantly. This behavior is well documented in reports on the compressive strength of horizontally cored first-year sea ice samples [Richter-Menge et al. (1986), Wang (1979), and Peyton (1966)]. The first-year sea ice tests have shown that the compressive strength of horizontal samples loaded parallel to the c-axes (σ:c = 0°) is greater than the strength of samples loaded perpendicular to the c-axes (σ:c =

90°) and that both are greater in strength than a sample where σ:c = 45°.

The Phase I and II unconfined, uniaxial compressive strength data is combined in a mean strength vs strain rate plot in Figure 6. We have noted the compressive strength of the horizontal and vertical samples at 10^{-4}/s separately in the figure. All of the test specimens used at the other test conditions were from vertically cored ice. We will compare the test results from the Phase I and II

7
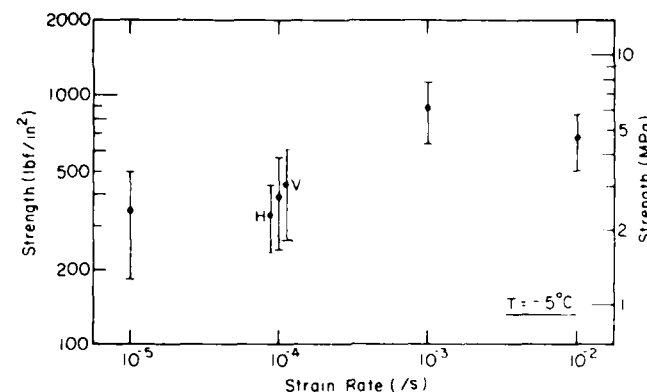
a. Samples tested at -5 °C.
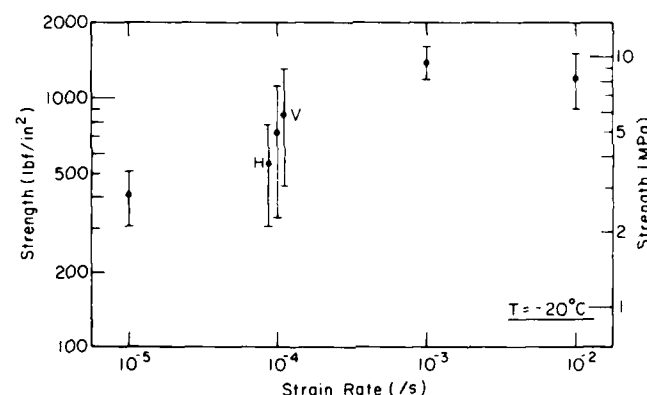
b. Samples tested at -20°C.

Figure 6. Unconfined, constant-strain-rate mean compressive strength vs strain rate. H = horizontally cored samples only, V = vertically cored samples only. The bars denote one standard deviation.

vertically cored samples only, since the orientation of the samples does affect the compressive strength.

As discussed in the Phase II report on test results (Cox et al. 1985), we would expect a power law relationship between the ice strength and strain rate in the ductile region between 10^{-5} and 10^{-3}/s (Mellor 1983). This relationship, which plots as a straight line on log-log paper, was not observed in our test results. The porosity variations between the Phase I and II samples appeared to explain this deviation. After analyzing the ice-structure characteristics of the samples tested in each group, however, it becomes apparent that variations in the overall structural composition of each test group also affect the test results.

The Phase I structural analysis indicated that, at -5°C, both the 10^{-3} and 10^{-5}/s sample groups were characterized by an isolated cluster of extremely high-strength columnar samples. These columnar samples were loaded such that $\sigma:z < 10°$. The two Phase I sample groups tested at -20°C did not exhibit this characteristic. The structural analysis of the Phase II ice samples tested at a strain rate of 10^{-4}/s (Fig. 5b and d) shows that at -20°C there is an isolated group of extremely high-strength columnar samples and at -5°C there is none. These differences are reflected in the mean strength vs strain rate plots. At -5°C (Fig. 6a), the mean strength of the 10^{-4}/s vertical samples falls below a straight line drawn between 10^{-5} and 10^{-3} test results of Phase I. The mean strength of the 10^{-4}/s

8

samples tested at -20°C lies above this line (Fig. 6b).

Variations in the structural composition of the -5 and -20°C, 10^{-2}/s tests are also likely to help explain the apparent decrease in strength relative to the tests done at 10^{-3}/s. We anticipated a leveling off in strength between 10^{-3} and 10^{-2} based on work by Richter-Menge et al. (1986) on first-year sea ice and by Blair (1986) on transversely isotropic columnar, saline ice grown in the laboratory. Unfortunately, only a few ice samples tested at 10^{-2}/s could be structurally analyzed since the majority of samples were destroyed during the tests. The ice fails in an explosively brittle manner at these test conditions. Thin sections of the end pieces taken immediately adjacent to the test specimen were subsequently lost due to melting during failure of the cold-storage room.

Confined constant-strain-rate compression tests

The confined or conventional triaxial constant-strain-rate compression tests were done using the triaxial cell developed in Phase I (Mellor et al. 1984). This triaxial cell was designed to ramp the radial confining pressure in constant proportion to the axial stress being applied; $\sigma_1 > \sigma_2 = \sigma_3$ and σ_2/σ_1 = constant. The Phase II confined compression tests were done at two temperatures (-5 and -20°C), two strain rates (10^{-3} and 10^{-5}/s), and two σ_2/σ_1 ratios (0.25 and 0.50). The axial stress and the radial stress are represented by σ_1 and σ_2, respectively. A total of 55 confined compression tests were completed. Plots of strength vs porosity that include the structural classification and crystallographic measurements of the tested ice samples are given in Figures 7a through f. In Table 4, we have summarized the percent granular, columnar, and mixed ice samples at each test condition.

The distribution of ice types at a given test condition is relatively consistent. The majority of samples consists of a mixture of columnar and granular ice, similar to the Phase I and Phase II unconfined compression test samples. There is one exception: at a strain rate of 10^{-5}/s, temperature of -5°C, and confinement ratio of 0.25, there are approximately the same number of samples in each ice type category.

We would anticipate the influence of ice structure in the confined compression tests to be similar to that observed in the unconfined compression tests given the common deformational mechanisms. In general, we did observe this to be the case. Columnar samples with a σ:z angle near 45° had a low compressive strength (Fig. 7a). There was an increase in strength as σ:z became greater than or less than 45°. The columnar and mixed ice samples from ridge B, which were used in half of these tests, tended to have a high σ:z angle. Consequently, we did not observe any isolated groups of high-strength columnar samples in the confined compression tests on the multi-year ridge samples. This should be noted when combining the results of the confined compression tests and the Phase I unconfined compression tests data to define the characteristics of the yield surface. Recall that in Phase I the columnar ice samples generally had low σ:z angles. As we discussed in the combined analysis of the unconfined compression test data from Phase I and II, differences in the overall ice-structure characteristics of the test groups do affect the relative mean strengths. Addition of the multi-year floe ice samples tested in Phase I at a confinement ratio of 0.46 does show that in the confined tests, columnar samples with a σ:z angle near 0° tend to have the highest strength (Fig. 7b and c).

Table 4. Summary of percent granular, columnar, and mixed ice samples at each Phase II confined compression test condition.

| σ_2/σ_1 = | -5°C | | | -20°C | | |
	0.25 10^{-5}/s	0.50 10^{-3}	0.50 10^{-3}	0.25 10^{-3}	0.50 10^{-5}	0.50 10^{-3}
Granular	30	11	22	22	11	11
Columnar	30	11	11	11	11	0
Mixed	40	78	67	67	78	89
Total samples tested	10	9	9	9	9	9

9
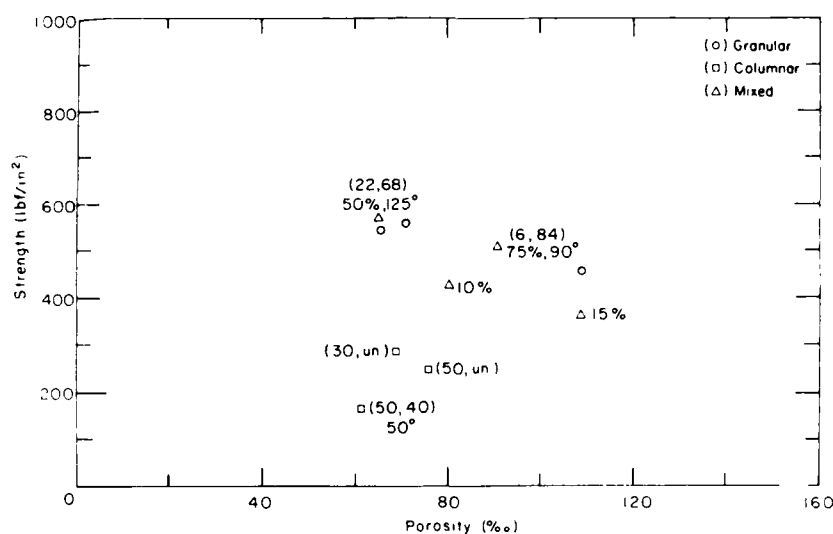
a. Phase II multi-year ridge samples tested at $10^{-5}/s$, $-5°C$, and $\sigma_2/\sigma_1 = 0.25$.

b. Phase II multi-year ridge samples (open symbols) tested at $10^{-5}/s$, $-5°C$, and $\sigma_2/\sigma_1 = 0.50$ and Phase I multi-year floe samples (closed symbols) tested at $10^{-5}/s$, $-5°C$, $\sigma_2/\sigma_1 = 0.46$.

Figure 7. Confined, constant-strain-rate compressive strength vs porosity for all Phase II ridge samples with the structural classification indicated for each sample. Phase I multi-year floe test data is included when appropriate. Crystallographic measurements indicated next to each sample: (σ:z, σ:c), % columnar, ° spread.
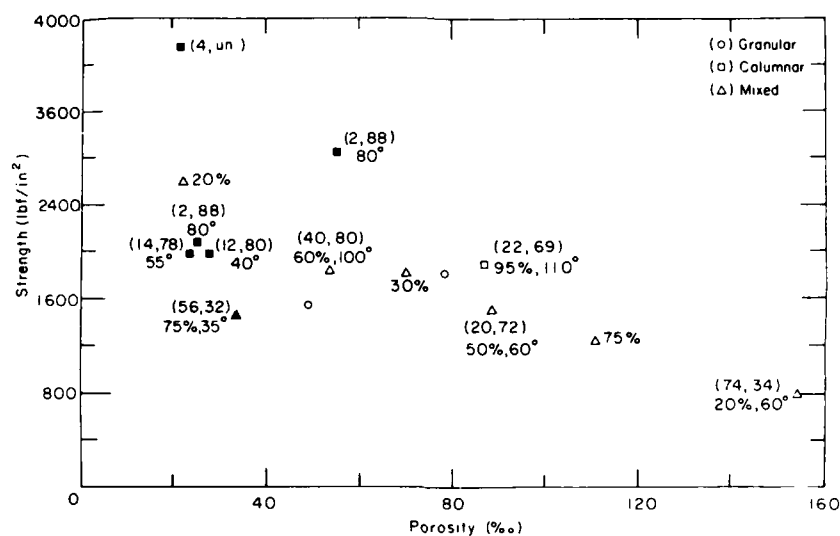
c. Phase II multi-year ridge samples (open symbols) tested at $10^{-3}/s$, $-5°C$, and $\sigma_2/\sigma_1 = 0.50$ and Phase I multi-year floe samples (closed symbols) tested at $10^{-3}/s$, $-5°C$, $\sigma_2\sigma_1 = 0.46$.
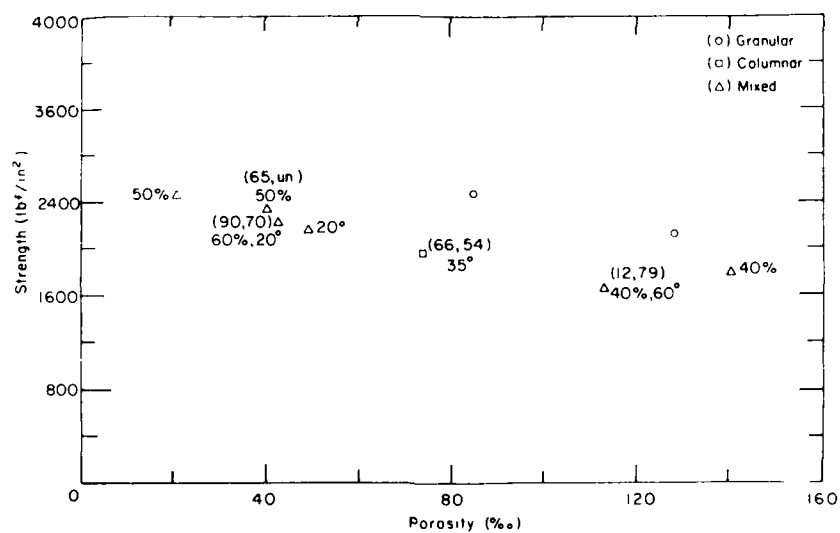
d. Phase II multi-year ridge samples tested at $10^{-3}/s$, $-20°C$, and $\sigma_2/\sigma_1 = 0.25$.

Figure 7 (cont'd).

11

e. Phase II multi-year ridge samples (open symbols) tested at $10^{-5}/s$, -20°C, and $\sigma_2/\sigma_1 = 0.50$ and Phase I multi-year floe samples (closed symbols) tested at $10^{-5}/s$, -20°C, and $\sigma_2/\sigma_1 = 0.46$.
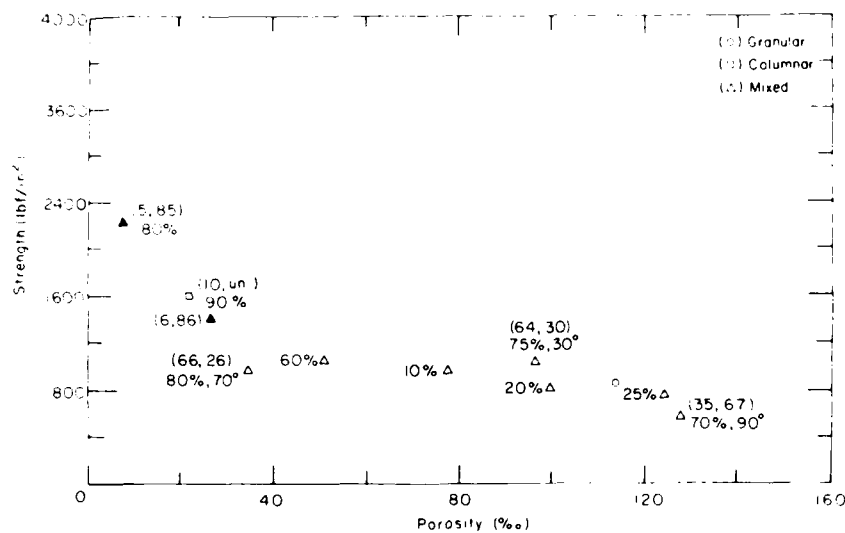
f. Phase II multi-year ridge samples (open symbols) tested at $10^{-3}/s$, -20°C, and $\sigma_2/\sigma_1 = 0.50$ and Phase I multi-year floe samples (closed symbols) tested at $10^{-3}/s$, -20°C, and $\sigma_2/\sigma_1 = 0.46$.

Figure 7 (cont'd). Confined, constant-strain-rate compressive strength vs porosity for all Phase II ridge samples with the structural classification indicated for each sample. Phase I multi-year floe test data is included when appropriate. Crystallographic measurements indicated next to each sample: (σ:z, σ:c), % columnar, ° spread.

12

The confined compressive strength of mixed and granular ice samples shows a strong tendency to decrease with an increase in porosity at all test conditions. Those mixed ice samples with a high percent of columnar ice (80% or more) lie on the outside of the strength vs porosity band. As we discussed in the previous section, this is a result of the orientation of the columnar fragments within the sample.

Uniaxial constant-strain-rate tension tests

Direct tension tests were done on 36 multi-year-ridge ice samples in Phase II of the program. All of these samples failed via an extension mechanism as illustrated in Figure 3d. Tensile strength is plotted against sample porosity in Figure 8. We have included the structural classification and crystallographic measurements for the samples in this figure.
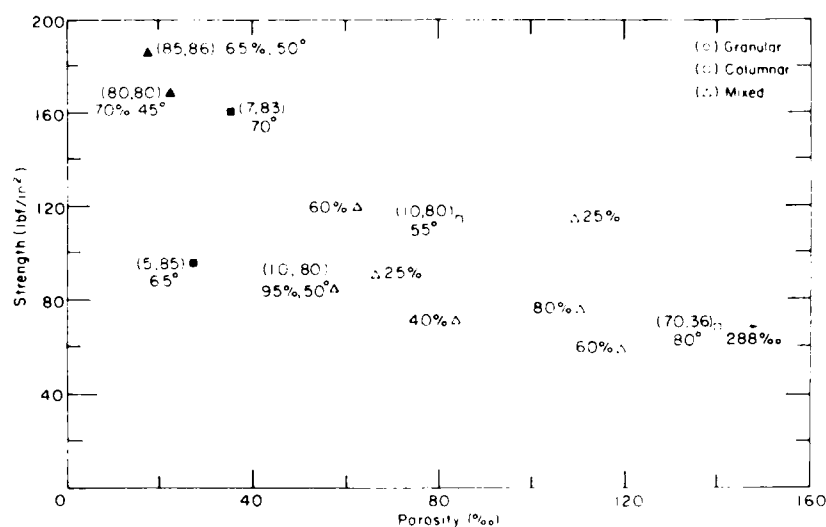
a. Samples tested at 10⁻³/s and -5°C.
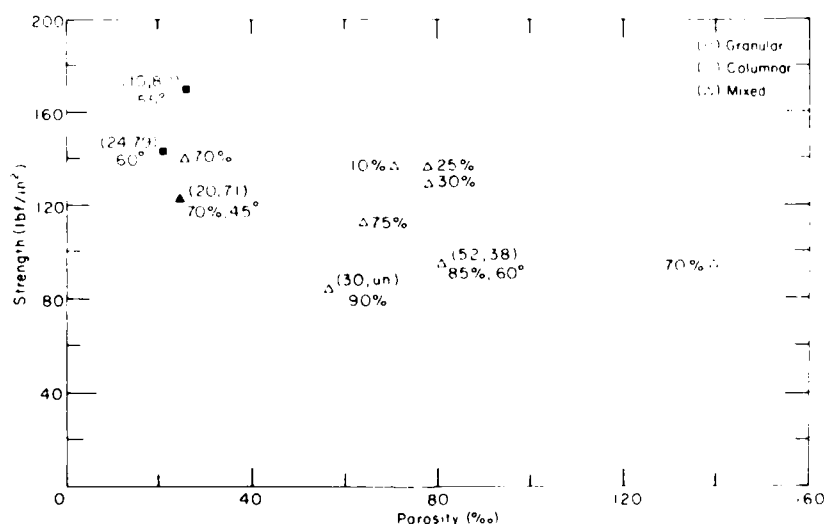
b. Samples tested at 10⁻⁵/s and -5°C.

Figure 8. Constant-strain-rate tensile strength vs porosity for all Phase II ridge samples with the structural classification indicated for each sample. Phase I multi-year floe test data is included and is indicated by a closed symbol. Crystallographic measurements indicated next to each sample: (σ:z, σ:c), % columnar, ° spread.

13
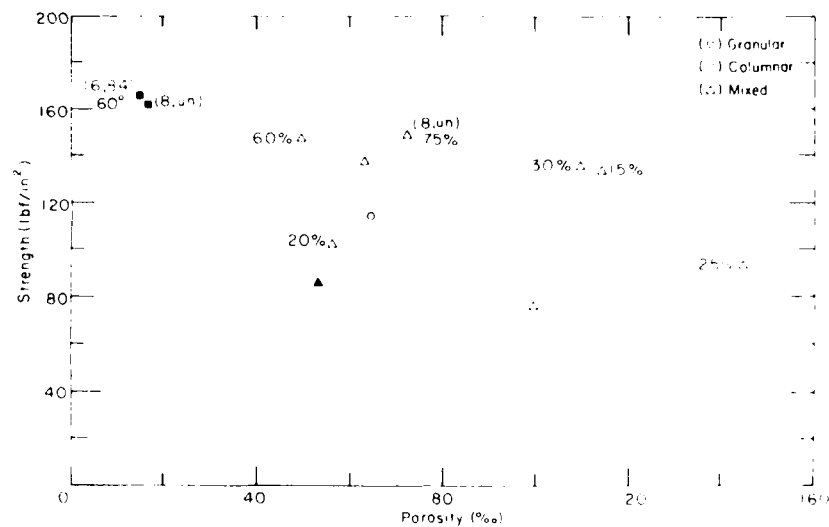
c. Samples tested at 10^{-3}/s and -20°C.
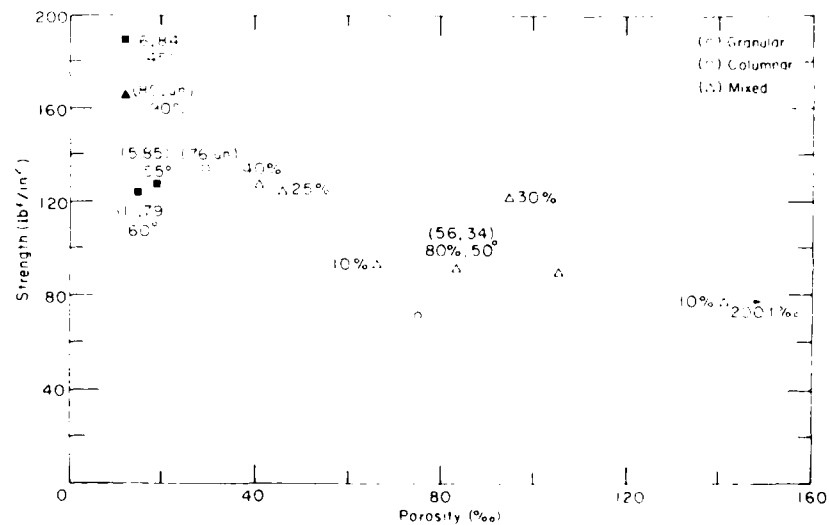
d. Samples tested at 10^{-5}/s and -20°C.

Figure 8 (cont'd). Constant-strain-rate tensile strength vs porosity for all Phase II ridge samples with the structural classification indicated for each sample. Phase I multi-year floe test data is included and is indicated by a closed symbol. Crystallographic measurements indicated next to each sample: (σ:z, σ:c), % columnar, ° spread.

All but six of the multi-year-ridge ice samples tested in tension consisted of a mixture of columnar and granular ice (Table 5). Three of the remaining samples were columnar and three were granular. To gain a more complete understanding of the influence of ice structure on the tensile strength of the multi-year ice, we have included the Phase I multi-year floe ice test results in Figure 8. The floe ice was predominately columnar. Based on the combined results, it appears that the tensile strength of multi-year ice shows little dependency on ice type. We do observe that the columnar ice samples tend to have a higher strength than the mixed and granular ice samples at all test condi-

Table 5. Summary of percent granular, columnar, and mixed ice samples at each Phase II uniaxial tension test condition.

	-5°C		-20°C	
	10^{-3}/s	10^{-5}	10^{-3}	10^{-5}
Granular	0	11	11	11
Columnar	22	0	0	11
Mixed	78	89	89	78
Total samples tested	9	9	9	9

tions. We believe that this is due to the generally lower porosity of these columnar samples rather than differences in the ice type. If the columnar structure of the ice was the reason for the increased tensile strength, we would expect to see a relationship between the orientation of the columns relative to the load (σ:z) and the strength. Such a relationship has been observed by both Peyton (1966) and Dykins (1970) in tests on first-year sea ice samples. In Peyton's test the tensile strength of the ice varied from 290 lb/in.^{2} at a σ:z orientation of 0° to 100 lb/in.^{2} at an orientation of σ:z = 90° and
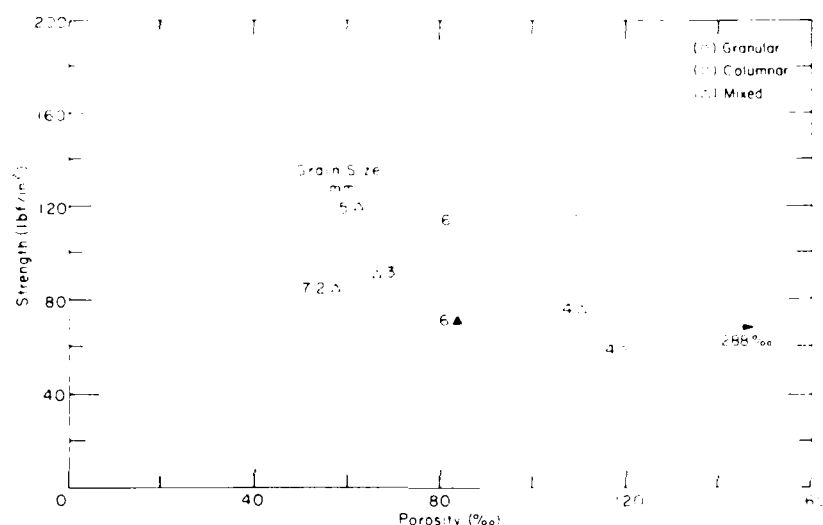
a. Samples tested at 10^{-3}/s and -5°C.
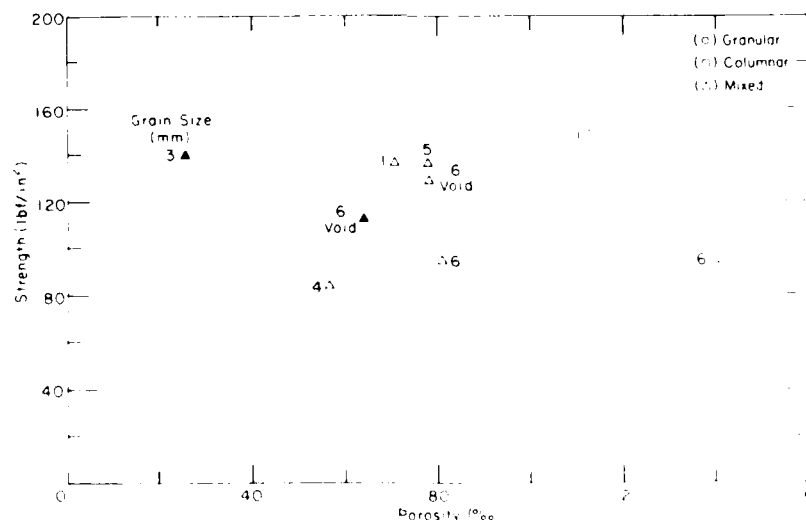
b. Samples tested at 10^{-5}/s and -5°C.

Figure 9. Constant-strain-rate tensile strength vs porosity for all Phase II ridge samples with the mean grain size (mm) at the failure plane indicated for each sample. Failure at an abrupt change in ice type is denoted by a closed symbol. Failure coincident with a void is also indicated.

15
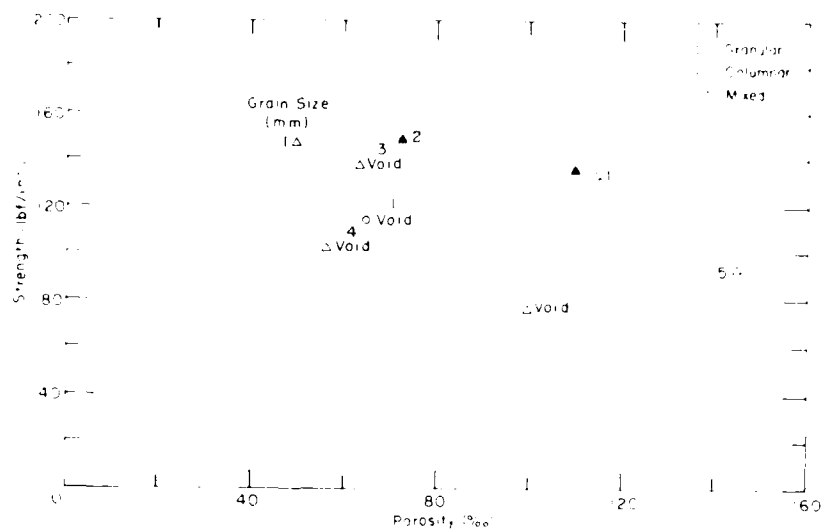
c. Samples tested at 10^{-3}/s and -20°C.
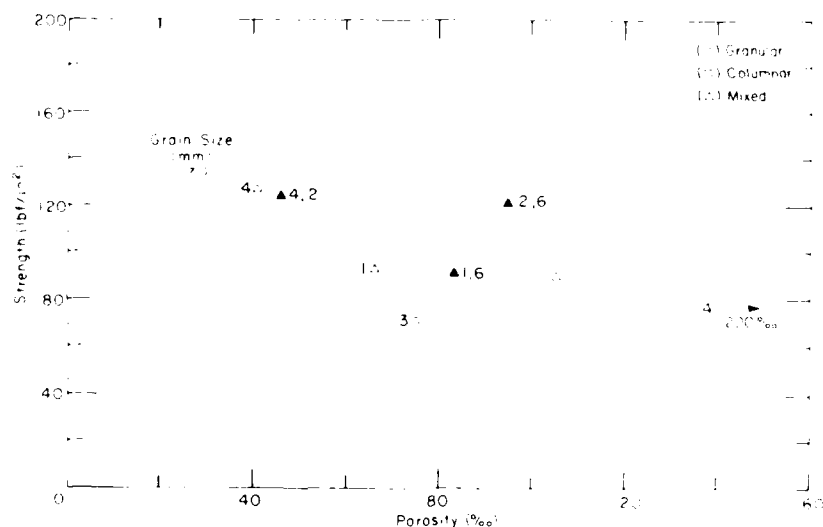
d. Samples tested at 10^{-5}/s and -20°C.

Figure 9 (cont'd). Constant-strain-rate tensile strength vs porosity for all Phase II ridge samples with the mean grain size (mm) at the failure plane indicated for each sample. Failure at an abrupt change in ice type is denoted by a closed symbol. Failure coincident with a void is also indicated.

$\sigma{:}c = 45°$. The tests by Dykins supported these findings. Our test data do not indicate this trend. We do note, however, that a columnar ice sample with a porosity comparable to a mixed or granular ice sample also has a comparable strength (Fig. 8a and d).

We also analyzed the effect of grain size on the tensile strength of the multi-year-ridge ice samples. In Figure 9, we have indicated the mean grain size measured at the failure plane for each test sample. Two values next to a data point indicate that the failure plane crossed both columnar and granular ice crystals. The larger number represents the mean columnar grain size and the smaller, the mean granular grain size. Results from direct tension tests on freshwater, equiaxed polycrystalline ice (Currier and Schulson 1982) show an inverse relationship between grain size and tensile strength.

16

This relationship was not apparent in our test results. We did observe a tendency for the mixed samples ice to fail in the part of the specimen where the grains were coarser. There were exceptions, including mixed ice samples with columnar fragments oriented in the hard fail direction (σ:z = 0°). These samples failed in the finer-grained ice that surrounded the fragments. Other mixed ice samples failed at abrupt changes in ice structure. One consistent observation was the coincidence of failure planes with large (> 1 cm), isolated voids in the samples. The samples that failed at structural discontinuities and voids are indicated in Figure 9.

It becomes apparent on these plots that while the location of the failure plane may be influenced by grain size, changes in the ice structure, and large voids, the tensile strength of the samples is not. Instead, the porosity of the sample seems to be the dominant characteristic influencing the tensile strength of the multi-year-ridge ice samples. This is true at all test conditions.

DISCUSSION

A total of 14 multi-year pressure ridges have been sampled in the course of this mechanical properties test program. We have structurally analyzed ice test specimens from 13 of these ridges. In Table 6, we list the number and percent of columnar samples tested in each of the ridges. We have included as columnar those mixed samples that are made up of 80% or more columnar ice. Our Phase I and II test results suggest that these mixed ice samples behave similarly to the columnar ice samples.

The amount of columnar ice varies from ridge to ridge. As we discussed in the Phase I ice structure analysis report (Richter-Menge et al. 1987), we believe this is due to differences in the mode of formation of the ridge. Ridges initially formed by the compression of one first-year ice sheet against another contain large blocks of columnar ice. The ice in a ridge formed by shearing, on the other hand, is highly fragmented. Samples taken from ridges should reflect these differences. We would expect to get a higher percentage of columnar samples from a multi-year pressure ridge formed by compression than from one formed in shear.

A frequency histogram of the number of columnar samples in a given σ:z orientation is presented in Figure 10. The frequency histogram of the Phase I columnar samples was originally present-

Table 6. Columnar ice samples tested in Phase I and II. These samples include both columnar and mixed samples with 80% or more columnar ice.

Ridge no.	Total samples tested	Total columnar samples	% columnar samples
		Phase I	
1	23	13	57
2	24	4	17
3	22	3	14
4	22	6	27
5	22	5	23
6	12	0	0
7	23	6	26
8	24	15	63
9	24	1	4
10	24	8	33
		Phase II	
A	46	1	2
B	54	9	17
C	53	20	38
Total	373	91	24
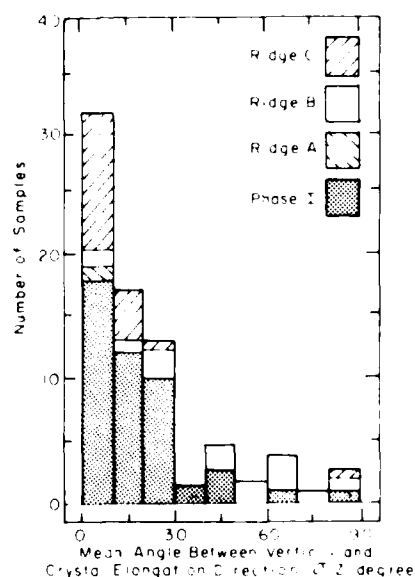
Figure 10. Frequency histogram of the Phase I and II columnar ridge ice samples in a given σ:z orientation.

17

ed and discussed in Richter-Menge et al. (1987). In that report we noted the relatively large number of low σ:z measurements. Based on this observation, we concluded that in the 10 ridges we sampled during Phase I the blocks of columnar, first-year sea ice that were incorporated into the ridge during its formation were lying in a near horizontal position. The vertically cored, columnar samples taken from these ridges tended to have a high compressive strength since they were loaded in the hard-fail direction (σ:z = 10°). We further anticipated that the mean compressive strength obtained from a series of tests on vertical ridge samples would be higher than the mean value obtained from horizontal samples. The horizontal columnar samples would tend to be loaded normal to the elongated crystal axis (σ:z = 90°), giving a lower compressive strength and, hence, a lower overall mean strength. The difference would be strongly dependent on the amount of columnar ice in the test series and the orientation of the columnar ice crystals.

Phase II unconfined compression tests on matched horizontal and vertical pairs collected during the second field program confirmed our hypothesis (Richter-Menge and Cox 1985). As we discussed earlier in this report, we found the effect of sample orientation on the mean compressive strength of multi-year-ridge ice samples tested at a given condition to be significant (Fig. 5b and d). The difference was greater in the test series with a higher percent of columnar samples (Fig. 5d).

The results of the compression tests on matched horizontal and vertical pairs would probably have been different, however, had we taken our samples from ridge B. The samples taken from this ridge tended to have a high σ:z angle, as indicated in Figure 10. Our compression test results on the ridge samples suggest that columnar samples with a σ:z angle near 45° are generally weaker than mixed or granular ice samples with comparable porosities. Columnar samples with 15° < σ:z < 35° or 55° < σ:z < 90° have strengths comparable to the mixed ice samples. We would therefore expect the mean compressive strength of vertically cored samples taken from ridge B to be comparable to the strength obtained from horizontal samples.

Based on our sampled ridge population, it still appears that the columnar blocks within a ridge tend to be in a near horizontal direction with the elongated crystal axis near vertical. The characteristics of the ridge B columnar ice samples show us, however, that this is not always the case. This ob-servation again points out the importance of the ice structure analysis for the interpretation of multi-year ice data. Each data group is unique with respect to the number of granular, columnar, and mixed ice samples and the orientation of the columnar ice within the samples. These variations in ice structure, combined with differences in porosity, will be reflected in the mean strengths. Without a thorough structural analysis of the ice types in all of the test groups, the combined results of a program could lead to erroneous conclusions. This is particularly true with respect to the compressive strength of the ice, both unconfined and confined. Our results on the strength of the multi-year-ridge ice samples loaded in tension suggest that, for strain rates from 10^{-5} to 10^{-3}/s and temperatures between –20° and –5°C, the tensile strength is insensitive to ice type. More tension tests should be done on ridge samples to confirm this observation, as we tested only nine samples at each test condition. This is an extremely small number of tests, given the variability of the material.

Ideally, we should be able to devise a system that allows us to adjust each data set to reflect the number of granular, columnar, and mixed ice samples that would be found in a 'representative' population of multi-year ridge samples. Orientation of the columnar ice samples would also have to be normalized. We would then be more certain of our conclusions made on the basis of combined data sets. It appears that this could be done by weighting the results of each test. The difficulty comes in defining the representative sample population. We expect it to be a function based on the number of ridges sampled and the number of samples taken from each ridge. Our current data set, involving data from 13 ridges, obviously is still too small to define this function with any certainty.

CONCLUSION

The ridge building process itself appears to be extremely dynamic, based on the large percentage (approximately 80%) of mixed ice samples in our combined Phase I and II data set. It also appears that there may be a preference for the columnar ice blocks in a ridge to lie in a near horizontal position. This results in a dependency between mean compressive strength and sample orientation. Vertically cored samples tend to give a higher mean compressive strength than horizontal samples.

At the end of the first phase of this testing program it had become apparent that the ice structure in multi-year ridge samples was extremely variable and that the structure had a profound effect on the mechanical properties of the ice. The Phase II test results confirm this observation.

The ice structure analysis of the Phase II unconfined and confined compression tests shows that the effect of ice structure on the compressive strength of multi-year ridge ice samples is independent of the temperature, strain rates, and confining ratios that we used in our test series. We will, therefore, restate the following general conclusions made in the Phase I report:

- For columnar ice samples, the dominant characteristic that influences sample strength is crystal orientation. Columnar samples with the direction of crystal elongation near vertical and with a high degree of crystal c-axis alignment will have extremely high compressive strengths. When the direction of crystal elongation coincides with the direction of maximum shear at an angle of 45° to the load, the columnar samples have a very low compressive strength.
- A sample composed of both columnar and granular ice (classified as a mixed ice sample) will exhibit mechanical properties that are similar to a columnar sample if it contains 80% or more columnar ice.
- The orientation of the columnar fragments in a mixed ice sample influences the overall compressive strength and deformational characteristics of the sample. If the columnar fragments are oriented in a hard fail direction the sample will have a relatively high strength. Failure in these samples will occur in the granular material surrounding the columnar fragments.
- Mixed and granular ice samples show a significant decrease in strength with an increase in ice porosity.

The tensile strength of the multi-year ridge ice samples does not appear to be significantly influenced by ice structure. Rather, the porosity of the sample is the dominant characteristic with respect to strength.

The most significant conclusion drawn from this study is the importance of characterizing the ice structure of each test specimen. It becomes apparent that the structural analysis is necessary for the proper choice and interpretation of constitutive parameters. Without such an analysis, the development of a constitutive law for multi-year ridge ice based on the data from mechanical property tests on ridge samples will be misleading. An ice structure analysis should become a standard procedure in all multi-year ridge programs. We also suggest the compilation of ice structure data taken in field sample and testing programs from all available sources. This would provide an opportunity to determine representative ridge characteristics and, hence, may lend insight toward the overall ridge mechanical properties that should be used in design codes.

LITERATURE CITED

Blair, S.C. (1986) Confined compressive strength of saline ice at intermediate strain rates. In *Proceedings of the Second Ice Penetration Technology Workshop, 16–19 June, 1986, Monterey, California.*

Cox, G.F.N., J.A. Richter-Menge, W.F. Weeks, M. Mellor and H. Bosworth (1984) Mechanical properties of multi-year sea ice. Phase I: Test results. USA Cold Regions Research and Engineering Laboratory, CRREL Report 84-9.

Cox, G.F.N., J.A. Richter-Menge, W.F. Weeks, M. Mellor, H.W. Bosworth, G. Durell and N. Perron (1985) Mechanical properties of multi-year sea ice. Phase II: Test results. USA Cold Regions Research and Engineering Laboratory, CRREL Report 85-16.

Currier, J.H. and E.M. Schulson (1982) The tensile strength of ice as a function of grain size. *Acta Metallurgica,* **30**: 1511–1514.

Dykins, J.E. (1970) Ice engineering: Tensile properties of sea ice grown in a confined system. Naval Civil Engineering Laboratory, Technical Report R689.

Jaeger, J.C. and N.G.W. Cook (1969) *Fundamentals of Rock Mechanics.* London: Methuen and Co., Ltd.

Langway, C.C. (1958) Ice fabrics and the universal stage. USA Snow, Ice and Permafrost Research Establishment, Technical Report 62.

Mellor, M. (1983) Mechanical behavior of sea ice. USA Cold Regions Research and Engineering Laboratory, Monograph 83-1.

Mellor, M., G.F.N. Cox and H.W. Bosworth (1984) Mechanical properties of multi-year sea ice: Testing techniques. USA Cold Regions Research and Engineering Laboratory, CRREL Report 84-8.

Peyton, H.R. (1966) Sea ice strength. Geophysical Institute, University of Alaska, Report UAG-182.

Richter-Menge, J.A. and G.F.N. Cox (1985) The

effect of sample orientation on the compressive strength of multi-year pressure ridge ice samples. In *Proceedings of the Conference Arctic '85, Civil Engineering in the Arctic Offshore, ASCE, San Francisco, California, 25–27 March 1985*, p. 465–475.

Richter-Menge, J.A., G.F.N. Cox, N. Perron, G. Durell and H.W. Bosworth (1986) Triaxial testing of first-year sea ice. USA Cold Regions Research and Engineering Laboratory, CRREL Report 86-16.

Richter-Menge, J.A., G.F.N. Cox and N.M. Perron (1987) Mechanical properties of multi-year sea ice. Phase I: Ice structure analysis. USA Cold Regions Research and Engineering Laboratory, CRREL Report 87-3.

Timco, G.W. and R.M.W. Frederking (1986) Confined compression tests: Outlining the failure envelope of columnar sea ice. *Cold Regions Science and Technology*, **12**(1986): 13–28.

Wang, Y.S. (1979) Crystallographic studies and strength tests of field ice in the Alaskan Beaufort Sea. In *Proceedings of the 5th International Conference on Port and Ocean Engineering under Arctic Conditions (POAC '79), Trondheim, Norway, 13–19 August*, **1**: 651–665.

APPENDIX A: MULTI-YEAR RIDGE SAMPLE DATA

This appendix contains the results from the ice structure analysis of the Phase II tests performed on multi-year-ridge ice samples. These tests included unconfined and confined constant-strain-rate compression tests and uniaxial constant-strain-rate tension tests. The test type is denoted by UC, CC, and UT, respectively. STR.CC.-3-5/ 0.5 indicates the structural analysis of the confined compression tests done at a strain rate of 10^{-3}/s, a temperature of $-5°C$, and a σ_2/σ_1 confinement ratio of 0.5. A similar strategy was used to identify all other test conditions. The parameters listed for each test are identified in Index A. The sample number RA01-262/289 gives the location and depth of the sample; that is, Ridge A, hole 1, at a depth of 262 to 289 cm. At a strain rate of 10^{-4}/s and temperatures of -5 and $-20°C$ in the unconfined compression tests, we tested matched pairs of vertically and horizontally cored ice samples. The vertical samples are labeled with a V and the horizontal samples with an H. All of the other samples in the Phase II portion of the test program were vertically cored.

INDEX A

Column number			
Compression	Tension	Symbol	Description
1	1	σ_m (lbf/in.^{2})	Peak stress or strength.
2	1	ϵ_m (GL) (%)	Strain at σ_m determined by DCDTs over a gauge length of 5.5 in. for the unconfined compression tests, 10.0 in. for the confined compression, and 4.5 in. for the tension tests.
3	3	t_m (s)	Time to peak stress.
4	4	E_i(GL) (10^4 lb/in.^{2})	Initial tangent modulus determined using strains found over the gauge length.
5	—	t_e (s)	Time to end of test.
6	—	σ_e/σ_m	Ratio of end stress at 5% full sample strain to peak stress.
7	5	n (%)	Sample porosity at test temperature.
8	6	Classification	Classification of ice texture type. 1 = granular, 2 = columnar, and 3 = a mixture of granular and columnar.
9	7	% columnar	Estimation of % columnar ice in the sample.
10	8	Min (mm)	Measurement of the minimum, maximum,
11	9	Max (mm)	and mean columnar grain size as measured
12	10	Mean (mm)	across the width of the grain.
13	11	σ:z (degree)	Angle between the direction of crystal elongation and the load applied along the cylindrical axis of the sample.
14	12	σ:c	Angle between the load and the mean crystal c-axis direction.
15	13	° spread	Degree of alignment of the c-axis. UN = unaligned, and R = random.
16	14	Min (mm)	Measurement of the minimum, maximum,
17		Max (mm)	and mean granular grain size.
18		Mean (mm)	
19	—	Type failure	Dominant failure mode. L = longitudinal splitting, S = shear, and MS = multiple shear failure.
20	17	Location	Location of failed area in sample. T = top, M = middle, and B = bottom of sample.

21

FILE STR.UC.-2-5

SAMPLE #	01	02	03	04	05	06	07	08	09	10	11	12	13	14	15	16	17	18	19	20
RA01-262/289	320	.10	.14	.709	.14	.591	64.1	3B	25	2	10	6				4	.5	1.5	S	T-M
RA0b-131/155	390	.05	.07	.735	.07		150.6	3	45										S	M
RA06-337/364	521	.07	.11	.869	.11		110.9	3											S	M
RC2y-112/13y	708	.07	.09	.942	.09		29.5	2A	100										S	T
RC2y-179/200	716	.08	.11	.974	.11		43.9	3A											S	B
RC29-342/369	470	.02	.08	.840	.08		67.1	3					9-70 / 30	30 / 70	27 (80%) / 20 (20%)-B				S	M
RC31-125/152	789	.03	.13	1.000	.13		50.7	3											S	M
RC31-197/224	645	.07	.12	.975	.12		68.8	3											S	T-M
RC31-270/305	951	.08	.12	.995	.12		27.5	2A											S	M

FILE STR.UC.-4-5

SAMPLE #	01	02	03	04	05	06	07	08	09	10	11	12	13	14	15	16	17	18	19	20
RC32-135/14?v	350	.15	16.50	.771	500	.591	76.3	3B	50									.5	MS	M
RC43-150H	324	.11	10.60	.736	500	.578	104.0	3B	20									.5	MS	M
RC33-205/232v	476	.10	7.80	.983	500	.433	70.6	3B	85	T-10 / B-9	1.5	65	28	90	20-T / UN-B			.5	MS	M
RC43-222H	402	.26	25.40	.871	500	.505	60.4	3	30										MS	M
RC46-047/073v	362	.09	7.10	.807	500	.362	63.3	3B	45	B-13	3	6	8	82	35-B	2			MS	M
RC44-073H	326	.09	5.90	.921	500	.377	86.2	3A	80	11	3	8	36	82	50				MS	M
RC44-06?H	227	.11	11.70	.639	500	.403	127.7	3	75	8	1	5	60	64	30		.5		MS	M
RC46-023/110v	500	.52	37.70	1.068	500	.309	66.7	3A	90	9	2	7	4	86	35				MS	M
RC44-066H	360	.11	9.80	.990	500	.245	25.8	2A	100	8	1	6	85	90	55				MS	M
RC46-147/175v	271	.15	14.00	.846	500	.424	69.7	3	85	10	2	7	10	80	30				MS	M
RC44-150H	175	.05	5.50	.834	500	.794	54.0	3A	90	9	2	7	78	30	15				MS	M
RC46-240/272v	446	.09	9.30	1.006	500	.428	75.5	3A	90	2	10	7	8	82	40				MS	T
RC44-255H	271	.03	4.60	.819	500	.410	56.4	3B	70										MS	T
RC47-025/053v	322	.10	9.00	.782	500	.394	81.1	3A	80	T-10 / B-10	3	9 / 6	0	90 / 90	55-T / 80-B				MS	M
RC45-040H	306	.04	6.30	.671	500	.363	142.2	2A	90	11	2	6	80	30	70				MS	M-B
RC47-191/217v	642	.11	6.00	1.144	500	.244	50.2	3A	90	10	2	7	5	83	25				MS	M-B
RC44-206H	561	.16	16.60	1.074	500	.265	46.7	3A	90	9	3	5	85	80	30				MS	M-B
RC47-275/302v	326	.17	18.50	.815	500	.377	59.9	2A	100	T-15 / B-17	3	8-T / 5-B	20		UN				S	M
RC44-283H	366	.12	15.00	.954	500	.445	73.5	3B	50									.5	MS	M

22

FILE STR.UC.-2-20

SAMPLE #	01	02	03	04	05	06	07	08	09	10	11	12	13	14	15	16	17	18	19	20
RA01-069/036	507	.03	.12	.765	.12		182.4	1										3.0	S L	T-M 2-8
RA01-C75/105	1150	.13	.16	.887	.16		126.9	3	30											2-8
RA01-339/369	1361	.13	.16	1.068	.16		37.5	39	50											
RA01-429/455	1470	.10	.17	1.024	.17		74.5	39												
RA06-058/085	971	.09	.13	1.522	.13		93.8	3										2.0		
RA06-266/293	1104	.13	.15	.882	.15		121.3	33									4.0	1.0	S	
RC29-251/273	1648	.13	.16	1.232	.16		27.0	3	80	3	12	5	T-70	78	26-T	1			S	B
RC31-350/377	1058	.09	.13	1.156	.13		70.6	3	40	3	13	9							S	M
RC31-416/443	1520	.17	.19	1.255	.19		14.1	2A												

FILE STR.UC.-4-20

SAMPLE #	01	02	03	04	05	06	07	08	09	10	11	12	13	14	15	16	17	18	19	20
RC32-231/253V	243	.21	22.50	1.237	500	.504	46.2	2A	100	15	3	10	15	76	55				MS	2-8
RC43-245H	544	.09	6.50	1.156	500	.306	29.9	2A	100	12	3	7	86	12	50				MS	
RC32-267/294V	541	.11	21.10	1.036	500	.253	42.1	2A	100	10	2	9	6	84	35				MS	
RC35-243/270V	896	.16	13.50	1.278			24.0	2A	100	12	1	9	8	84	50				MS	
RC43-243H	708	.11	9.70	1.490	500	.202	78.5	2A	100	18	2	10	90	5	30				MS	
RC32-303/323V	575	.11	11.70	.876	500	.389	64.1	78	40	5	2	5							MS	
RC43-316H	542	.07	6.20	1.191	500	.675	29.8	2A	100	9	4	7	85	25	30			.5	MS	
RC32-345/372V	485	.17	27.90	.776	500	.361	98.5	3	90	6	2	5							MS	2-8
RC43-357H	597	.14	14.40	.965	500	.400	58.7	78	40	14						1		1.0	MS	2-8
RC35-242/268V	947	.19	19.40	1.287	500	.307	70.1	2A	100	14	2	8	10	82	60				MS	
RC43-257H	541	.10	11.00	1.144	500	.263	24.4	2A	100	8	1	7	85	5	40				MS	
RC33-363/395V	939	.18	14.20	1.101	500	.239	40.6	3	85	7	2	5						.5	MS	
RC43-331H	347	.13	14.30	1.176	500	.315	31.0	38	75	5	2	4					.5	.5	MS	
RC46-121/147V	517	.10	10.50	.101	500	.315	72.1	38	50	10									MS	2-8
RC46-123H	255	.08	9.50	.957	500	.592	28.4	2A	100	12	2	7	65	24	50				MS	2-8
RC46-173/199V	495	.11	12.10	.877	500	.355	70.4	38	40	11	1	7	90	20	40				MS	T
RC44-136H	1015	.13	12.40	1.292	500	.207	31.6	38	95	11	2	8	0	90	30				MS	
RC46-276/303V	620	.12	13.40	.952	500	.355	68.7	38	40	10	3	7	2	88	40				MS	T-M
RC44-299H	600	.12	15.50	.990	500	.442	48.9	38	30	8	3	8	90	35	30				MS	T-M
RC47-090/116V	1747	.19	20.70	1.311	25.70		41.0	2A	100	10	1	7	2	88	30				L	T-M
RC44-103H	505	.10	7.30	1.101	500	.336	34.8	2A	100	12	1	7	90	20	40				MS	
RC44-116H	243	.07	4.60	.921	500	.457	25.3	2A	100	11	2	8	90	25	45				MS	
RC47-127/153V	1346	.18	14.60	1.406	14.60		25.2	2A	95	10	3	7	2	89	40				MS	T
RC44-141H	267	.04	0.30	.896	500	.470	4.7	2A	100	11	3	8	90	35	30				MS	
RC47-300/322V	375	.11	10.00	1.352	500	.292	15.0	3	75	8	3	5	90	0	15				MS	T-M

FILE STR.CC.-5-5/0.5

SAMPLE #	01	02	03	04	05	06	07	08	09	10	11	12	13	14	15	16	17	18	19	20
RA10-005/055	723	.23	2.60	.221	50.00	1.000	155.7	3	20			6	B-74	34	60-B	3	.5	1.0	MS	M-B
RA10-442/017	1650	.50	5.40	.310	50.00	.742	68.2	39	30							3	.5	1.0	MS	T
RA11-233/250	1564	.44	4.20	.351	50.00	.634	96.7	3	50	9	2	7	20	72	60	4	1.0	1.0	MS	T-M
RB13-235/313	1870	.41	4.00	.454	50.00	.766	52.2	38	60					60	100	3	.5	1.0	MS	M
PB16-124/151	1926	.52	4.70	.376	50.00	.502	85.3	24	95	12	4	8	40	69	110				MS	M
PB16-262/233	1264	.35	3.10	.370	50.00	.554	108.9	3	75				22		T-10 B-T		2	1.0-T B-B	MS	M
PB17-235/453	1535	.42	3.90	.438	50.00	.775	76.8	1								2	.5	1.0	MS	M
PB17-247/234	1596	.40	5.60	.264	50.00	.809	43.1	1								5	1.0	2.0	MS	M
RB17-399/420	2402	1.01	10.60	.258	50.00	.694	23.6	38	20							2	.5	1.0	MS	M

FILE STR.CC.-5-5/0.25

SAMPLE #	01	02	03	04	05	06	07	08	09	10	11	12	13	14	15	16	17	18	19	20
RA06-134/161	457	.94	030	.172	5000	.783	107.9	1	10							5	.5	1.0	MS	M
RA06-186/163	427	.79	750	.767	5000	.726	79.3	3	15			3				4	.5	1.0	MS	T-M
RA06-199/220	370	.72	760	.162	5000	.891	107.5	3	75	7	2	4	6	84	90	6	.5	1.0	MS	M-B
RA08-259/286	515	.59	560	.408	5000	.549	89.4	3	50	10	2	7	22	68	125	4	.5	2.0	MS	M
RA08-290/517	575	.76	320	.291	5000	.702	64.3	3	100			5	50	40	50		1.0	2.0	MS	T-M
RB12-077/104	166	.36	342	.217	5000	.904	60.6	24								3	.5	1.0	MS	M
RB12-143/190	655	1.00	999	.306	5000	.670	70.2	1		5	2	4	30		UN	3	.5	1.0	MS	M
RB12-194/221	540	1.00	999	.245	5000	.685	65.3	1	100										MS	M
RB15-045/063	296	.49	444	.176	5000	.304	67.7	24	100			5	50		UN					
RB13-097/124	453	.39	790	.194	5000	.794	75.2	24	100											

FILE STR.CC.-5-5/0.5

SAMPLE #	01	02	03	04	05	06	07	08	09	10	11	12	13	14	15	16	17	18	19	20
FA10-276/243	>530	>5.00	>500	.172	5000	.371	176.3	3	15							4	.5	1.0	MS	M-B
RA10-372/350	557	1.32	1340	.330	5000	.991	203.8	1				4		78	55	3	.5	1.0	MS	M
RA10-459/466	446	2.51	2310	.267	5000	.921	104.3	38	20	7			12	60	UN	3	.5	1.0	MS	M
FA10-533/363	305	.96	960	.297	5000	.716	32.3	3	65		2	6	60		55	3	.5	1.0	MS	T
RB13-225/232	562	.65	650	.212	5000	.967	62.3	3	80			3	52	60	60	2	.5	1.0	MS	M
RB16-330/357	490	.73	730	.200	5000	.679	93.2	38	40	7	2	5	80	23	25	2	.5	1.0	MS	M
RB16-353/357	550	.91	910	.362	5000	.943	58.0	3	60				T-68	39	25-T	2	.5	1.0	MS	T-M
RB17-367/374	577	.30	910	.287	5000	.910	27.9	38	40	T-8 B-8		T-8 B-8	12	78	30				MS	M-B
RB17-463/470	250	.52	540	.436	5000	.652	25.2	24	90	2	2	3-T B-8								

24

FILE STR.CC.-3-20/0.25

SAMPLE #	01	02	03	04	05	06	07	08	09	10	11	12	13	14	15	16	17	18	19	20
RA08-025/052	2125	.51	6.00	.482	50.00	.524	128.0	1	50	9						3	.5	1.0	MS	T
RA08-340/347	2467	.70	7.20	.334	50.00	.403	21.4	38	40	6	1	5	12	79	60	7	1.0	2.0	MS	M
RA11-072/105	1679	.46	4.60	.420	4.60		112.7	38	40		1	4				3	1.0	2.0	S	M
RA11-127/154	1592	.47	4.90	.470	50.00	.404	140.4	33	40			6				2	.5	1.0	MS	T
RB16-132/159	2475	.65	6.40	.555	50.00	.431	94.8	1								4	1.0	2.0	MS	M
RB12-326/353	2157	.61	6.30	.397	50.00	.476	49.3	38	20							5	.5	1.0	MS	M
RB12-047/074	1974	.61	5.10	.546	50.00	.399	73.9	2A	100			7	66	54	35		1.0		S	T-M
RB12-239/266	2236	.52	5.70	.589	50.00	.416	42.4	38	60		2	6	90	70	20	4	1.0	2.0	MS	M-B
RB13-156/183	2332	.69	6.90	.534	50.00	.440	40.4	38	50		3	7	65		UN	3	1.0	1.0	MS	T-M

FILE STR.CC.-3-20/0.5

SAMPLE #	01	02	03	04	05	06	07	08	09	10	11	12	13	14	15	16	17	18	19	20
RA10-194/221	2674	.61	5.40	.830	50.00	.700	98.4	3	10	8	2	6	10	80	80	4	.5	1.0	MS	M-B
RA10-341/368	2574	.70	7.80	.680	50.00	.760	103.5	3	10	9	2	5	86	19	40	2	.5	1.0	MS	M
RA10-367/394	4011	.88	8.50	1.021	50.00	.547	18.0	3	40	B-9	2	7	8		UN-B	3	.5	1.0	MS	M
RB13-225/252	3009	.63	6.60	.901	50.00	.481	39.9	3	90	5	2	3						3.0	MS	T
RB13-342/369	4534	1.00	9.40	.936	50.00	.657	33.2	3	40		2	3							MS	M-B
RB16-089/116	2374	.49	4.50	.839	4.50		85.0	3	15		2	4				4	.5	1.0	MS	M
RB16-392/419	3029	.71	9.00	.860	50.00	.544	22.6	3	50							3	.5	2.0	S	T89
RB17-052/079	1210	.21	2.00	.639	2.00		46.7	1					7	83	30	3	1.0	1.0	MS	B
RB18-363/390	5602	1.20	12.00	1.000	50.00	.523	14.8	3	60			4								

FILE STR.CC.-5-20/0.5

SAMPLE #	01	02	03	04	05	06	07	08	09	10	11	12	13	14	15	16	17	18	19	20
RA10-090/117	>740	>5.00	>5000	.703	5000		123.5	3	25	12	2	4	64	30	30	4	.5	1.0	MS	M
RA10-133/160	851	1.52	1530	.479	5000	1.000	112.9	1	10	8	3	8	35	67	90	3	.5	1.0	MS	T-M
RA11-266/293	1030	.70	710	.297	5000	.743	95.9	3	75	8	3	6				3	.5	1.0	MS	M-B
RB16-156/185	>573	>5.00	>5000	.282	5000		127.1	3A	70	T-8 / 8-6	2	4-T / 3-B					.5	1.0	MS	T-M
RB16-198/215	820	1.01	1030	.300	5000	1.000	99.0	3	20							7	.5	1.0	MS	M
RB16-361/388	971	.78	750	.318	5000	.836	33.9	3	80	8	1	4	10	26	70			2.0	MS	M-B
R316-432/459	1600	.68	670	.452	5000	.592	21.7	2A	90	8	1	4	10		UN				S	T
R617-191/218	963	1.39	1380	.386	5000	.975	77.1	3	10							4	.5	1.0	MS	T-M
RB17-335/362	1050	1.10	1110	.391	5000	.910	50.4	38	60							3	.5	1.0	MS	M

FILE STR.UT.-3-?

SAMPLE #	01	02	03	04	05	06	07	08	09	10	11	12	13	14	15	16	17
RA03-073/105	115.0	.013	.32	.913	107.7	38	25		2 2	6-A 7-B	10	80	55				B
RA07-146/176	115.0	.011	.33	1.124	97.4	24	100	A-10 B-10		6							T
RA07-243/280	71.5	.008	.26	.943	91.0	3	40			6				5	1.0	2.0	T
PA14-55/85	70.0	.009	.26	.945	109.2	38	80							5	2.0	4.0	T
PA14-265/290	120.0	.012	.33	1.054	60.9	38	60			5				6	1.0	3.0	T
RB20-034/060	40.4	.007	.23	.977	118.8	38	60	6	2	4				0	1.0	3.0	B
RB20-161/188	91.5	.009	.27	.931	65.5	3	25							3	1.0	2.0	B
RB20-193/220	54.2	.007	.25	1.207	57.0	3	95	12	2	7	10	80	50				B
RB221-005/032	62.0	.011	.27	.616	258.0	24					70	36	90				B

FILE STR.UT.-?-5

SAMPLE #	01	02	03	04	05	06	07	08	09	10	11	12	13	14	15	16	17
RA07-1-1/24	125.0	.013	.03	.613	77.0	38	25	7	2	5				2	1.0	2.0	B
RA09-276/163	147.0	.012	21.60	1.150	112.6	1	70	4-7	2	5-A	52	38	40	7	1.0	1.0	T
RA09-261/371	115.0	.010	20.40	1.020	24.7	3	85	10	3	6	52	38	40		1.0	3.0	B
RB20-104/156	64.0	.014	14.00	.090	80.5	3	75	11	3	6	30		UN			4.0	T
RB21-146/191	115.0	.009	16.80	.436	64.2	38	90	10	2	4	30		UN				M
RB21-147/093	82.1	.010	32.30	.887	56.5	3	10							6	.5	1.0	T
RB21-217/244	115.0	.012	25.30	.917	70.2	3	70		2	4	70	40	40	3-2			M
RB26-013/045	54.6	.021	24.90	.786	139.1	3	70	0		6	20	20	UN		.5	1.0-A	B
RB26-165/191	135.1	.001	17.00	.940	78.1	2	70										

FILE STA.DT.(1758)

SAMPLE #	01	02	03	04	05	06	07	08	09	10	11	12	13	14	15	16	17
1403-042/...	125.	.012	.31	1.056	92.2	38	70								.5	1.0	B
1403-127/14	151.0	.012	.30	.967	152.6	38	15							5	1.0	7.0	a
1409-034/061	42.0	.009	.25	.955	92.5	3								10	2.0	5.0	B
1814-120/055	2.0	.009	.16	1.002	126.0	3	75			6				3	.5	1.0	6
1814-034/061	173.0	.012	.21	1.177	44.0	38	40			4-3	8		UN		.5	2.0	T
1830-062/115	73.0	.012	.32	1.158	44.2	3	75	8-13	3	4				5	.5	2.0	T
1830-144/032	32.0	.009	.27	1.117	50.0	3	20	8	3					5	1.0	3.0	R
1-81-301/7.4	154.0	.012	.32	1.072	50.1	3								4	.5	1.0	T
1-92-150/157	172.0	.010	.31	1.045	57.0	1											

FILE STB.DT.(1758)

SAMPLE #	01	02	03	04	05	06	07	08	09	10	11	12	13	14	15	16	17
1403-142/01.	33.0	.015	9.20	1.134	45.0	3	15							0	.5	1.0	a
1403-042/072	163.0	.014	14.10	1.011	94.3	38	70			6	56	34	50	5	1.0	2.0	M
1403-041/045	175.0	.014	15.50	1.046	40.0	3	40			4				4	1.0	2.0	R
1407-085/082	2.0	.014	14.60	.404	200.1	3	10			6						2.0	T
1410-152/159	6.0	.011	12.10	.907	92.6	3	80	17	3	6	56			4	1.0	1.0	8
1430-160/157	75.0	.012	12.30	.768	104.5	3							UN				
1814-145/216	71.4	.009	10.60	.910	74.3	1	100	17	3	7	76			4	1.0	3.0	T
1814-160/025	173.0	.009	24.50	1.036	28.8	38	25			4				4	1.0	2.0	B
1830-071/025	164.0	.012	15.30	1.006	45.6	38											

27

END

DATE

FILMED

8-88

DTIC